

AN ABSTRACT OF THE THESIS OF

Thanasarn Khuayjarernpanishk for the Master of Science  
(Name) (Degree)

in Civil Engineering presented on 9 April 1971  
(Major) (Date)

Title: Stress-Strain-Time Relations for a Compacted Residual Soil

Redacted for privacy

Abstract approved: \_\_\_\_\_  
Dr. W. L. Schroeder

The directional nature of the stress-strain-time relationship was investigated using linear shrinkage tests and one-dimensional compression. The samples for both tests were trimmed from specimens which were compacted at three percent above standard optimum moisture content. Pressure was applied at various angles from the compaction direction to determine the relationship between the compressive strains and test direction. The results from both tests supported the conclusion of isotropic behavior of the soil.

In the studies of stress-strain-time behavior the soil was represented by a mechanical model consisting of a spring and dashpot connected in parallel (the Kelvin model). Calculations were made for spring and dashpot constants. The test results show that the variation of the spring constant is pressure dependent and that the dashpot constant varies with time. The dashpot constant was independent of pressure.

The soil strains can be predicted with the following two equations.

$$\eta = A \left( \frac{t}{t_A} \right) \tan \theta$$

and

$$\epsilon = \frac{\sigma - \eta \frac{\sigma}{\epsilon}}{K}$$

Stress-Strain-Time Relations for a Compacted Residual Soil

by

Thanasarn Khuayjarernpanishk

A THESIS

submitted to

Oregon State University

in partial fulfillment of  
the requirements for the  
degree of

Master of Science

June 1971

APPROVED:

Redacted for privacy

\_\_\_\_\_  
Associate Professor of Civil Engineering  
in charge of major

Redacted for privacy

\_\_\_\_\_  
Head of Department of Civil Engineering

Redacted for privacy

\_\_\_\_\_  
Dean of Graduate School

Date thesis is presented

7 April 1971

Typed by Muriel Davis for

Thanasarn Khuayjarernpanishk

## ACKNOWLEDGMENT

The author is greatly indebted to his parents for their support throughout his education.

Special thanks are due Dr. W. L. Schroeder for his patience, advice, suggestions, and assistance in directing the research and writing of this thesis. Thanks are also extended to Dr. J. R. Bell for his advice and to Mr. Arlan H. Rippe for his assistance in writing the computer program.

## LIST OF TERMS

<u>Term</u>		
A	Interception of $\log \eta$ - $\log t$ plot on $\log \eta$ axis	$\frac{\text{kg.}}{\text{cm.}^2 \cdot \text{min.}}$
$C_c$	Compression index	dimensionless
D	Deviator stress	$\frac{\text{kg.}}{\text{cm.}^2}$
e	Void ratio	dimensionless
$\Delta H$	Deformation of one-dimensional compression sample	inch
$H_i$	Initial height of test samples	inch
K	Spring constant	$\frac{\text{kg.}}{\text{cm.}^2}$
$\Delta L$	Axial shrinkage of samples from shrinkage tests	inch
$L_i$	Initial height of shrinkage samples	inch
$R_{24 \text{ hr.}}$	Dial reading at 24 hour after pressure applied	inch
$R_i$	Initial dial reading for first load increment	inch
$R_f$	Final dial reading for last load increment	inch
t	Instantaneous time	minute
$t_A$	Time at $\eta = A$	minute
w	water content or moisture content	percent
$\epsilon$	Axial strain	percent
$\frac{\circ}{\epsilon}$	Rate of strain	per minute
$\eta$	Dashpot constant	$\frac{\text{kg.}}{\text{cm.}^2 \cdot \text{min.}}$

$\alpha$	Angle between test and compaction directions	degrees
$\tan\theta$	Slope of plot between $\log\eta$ and $\log t$	dimensionless
$\sigma$	Applied stress	$\frac{\text{kg.}}{\text{cm.}^2}$
$\sigma'_c$	Apparent precompression pressure of test sample	$\frac{\text{kg.}}{\text{cm.}^2}$

## TABLE OF CONTENTS

	<u>Page</u>
INTRODUCTION	1
THEORY	3
Effect of Orientation of Particles on Soil Behavior	3
Properties of Compacted Soil	5
Compaction	5
Structure of Cohesive Soil after Compaction	5
Effect of Soil Structure on Soil Properties	6
Effect of Mode of Compaction	7
Influence of Compaction on Compressibility of Soil	9
LABORATORY STUDIES	12
General	12
Test Procedure	14
Linear Shrinkage Test	14
One-dimensional Compression Test	16
TEST RESULTS	19
DISCUSSION OF RESULTS	26
Linear Shrinkage Test Results	26
One-dimensional Compression Tests	27
Relation between $C_c$ and $\alpha$	27
Stress-strain-time Relationship	28
CONCLUSIONS	36
BIBLIOGRAPHY	37
APPENDIX	39

## LIST OF FIGURES

<u>Figure</u>		<u>Page</u>
1	Structure of natural cohesive soil.	4
2	Effects of compaction on structure.	6
3	Dynamic compaction curves for a silty clay.	8
4	Static compaction curves for a silty clay.	8
5	Effect of one-dimensional compression on soil structure.	11
6	Test sample orientation.	13
7	Moisture density relationship.	15
8	Shrinkage measurement device.	17
9	Conbel compression machine .	17
10	Mechanical model representing soil behavior .	18
11	Linear shrinkage test results.	20
12	Axial strain versus pressure curves.	21
13	Variation of compression index and apparent precompression pressure with test direction.	22
14	Variation of strain from shrinkage and one-dimensional compression tests with direction of compression .	23
15	Spring constant variation with pressure.	24
16	Dashpot constant variation with time.	25
17	Strain rate versus time relationship from one-dimensional compression test.	32
18	Variation of strain rate with stress of constant time.	33

<u>Figure</u>		<u>Page</u>
19	Strain rate-time relationship.	34
20	Influence of creep stress intensity on creep rate.	35

# STRESS-STRAIN-TIME RELATIONS FOR A COMPACTED RESIDUAL SOIL

## INTRODUCTION

The arrangement of soil particles influences the engineering behavior of soil. This arrangement of soil particles is an important determining characteristic of soil behavior. In most problems in soil mechanics the soil is assumed to behave isotropically. The soil may behave isotropically or anisotropically depending at least partly on the orientation of the particles. The methods available for a direct study of soil fabric are necessarily very limited because of the small size of the soil particles involved. One can use electron microscopy and other such delicate techniques as the study of thin sections. Other methods available for the indirect determination of soil fabric rely upon measurement of soil properties which vary with structure. The term soil structure refers to the orientation and distribution of particles in the soil mass and the forces between adjacent soil particles. Soil structure may be deduced using various properties as indices, such as swelling and shrinking, compressibility, thermal conductivity, and shearing strength.

The purpose of this investigation was to determine if a compacted soil (MH-Gate Creek Soil) behaves isotropically. An investigation was performed by measuring the shrinkage of cubical samples

cut from compacted specimens. Also, the compressibility of the soil, for various directions of compression, was determined by performing one-dimensional compression tests with the samples compacted at three percent above optimum water content. Further, the stress-strain-time relations for the test specimens were observed and rheological constants for a Kelvin model were obtained.

The results of the laboratory study show that the soil behaves isotropically. The spring constant in the Kelvin model varies only as the applied pressure. The  $K\text{-log}\sigma$  curves have a shape similar to that of the  $e\text{-log}\sigma$  curves from one-dimensional tests. The dash-pot constant varies as elapsed time but not with applied pressure.

## THEORY

### Effect of Orientation of Particles on Soil Behavior

In cohesive soil the structure is determined largely by the clay minerals and the forces acting between them. The term soil structure refers to the orientation and distribution of particles in soil mass and the forces between adjacent soil particles. The force component of soil structure refers primarily to those forces that are generated within the particles themselves--electrochemical forces. Fabric is different from structure in that it is characterized only by soil particle arrangement.

The two extremes in soil structure, as illustrated in Figure 1, are flocculated structure and dispersed structure. In the flocculated structure the soil particles are edge to face and attract each other. A dispersed structure, on the other hand, has parallel particles which tend to repel each other. Between the two extremes there is an infinite number of intermediate stages. At the present development of knowledge and of techniques for measuring orientations and interparticle forces, there seems little justification in attempting to define structures between the two extremes. Thus the terms flocculated and dispersed are used in a general sense to describe soil elements which have the structures approaching those shown in Figure

1 (3). A discussion of forces between particles and introduction to the concepts of flocculated and dispersed structure may be found in Lambe (2).

The engineering behavior of a soil element depends very much on the existing structure. In general, an element of flocculated soil (isotropic) has a higher strength, lower compressibility, and higher permeability than the same element of soil at the same void ratio but in a dispersed state (anisotropic). The higher strength and lower compressibility in the flocculated state result from the interparticle attraction and the greater difficulty of displacing particles when they are in a disorderly array. The higher permeability in the flocculated soil results from the larger channels available for flow. Whereas a flocculated element and a dispersed element at the same void ratio have approximately the same total cross-sectional area available for flow, in the flocculated soil the flow channels are fewer in number and larger in size. Thus there is less resistance to flow through a flocculated soil than through a dispersed soil.

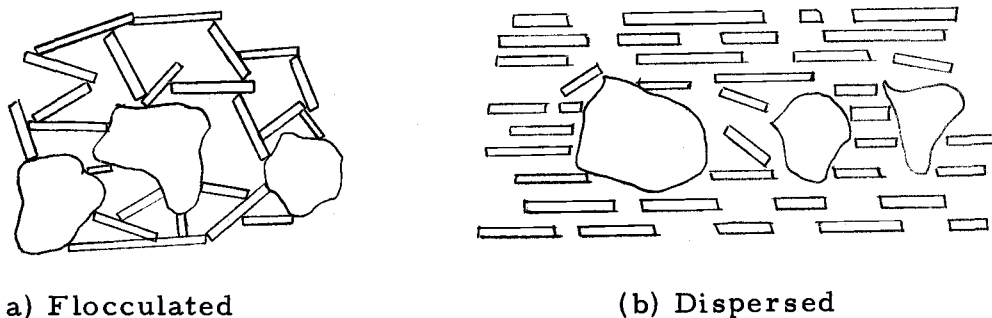


Figure 1. Structure of natural cohesive soil.

## Properties of Compacted Soil

### Compaction

The process of densifying, i. e., compacting, soil is the oldest and most important method of soil stabilization. Compaction alone will often solve a particular soil problem and is usually the most economical of the techniques available. In addition to being used alone, compaction constitutes an essential part of a number of the other methods of stabilization.

In compacting any particular soil, the engineer can vary moisture content, amount of compaction energy, and type of compaction. The characteristics of compacted cohesive soil will be discussed below.

### Structure of Cohesive Soil after Compaction

The influences that govern the initial soil structure of compacted cohesive soil at a given density are molding water content and method of compaction. Previous work (8) has shown that the structure of soil on the dry side of optimum is always flocculated no matter by which method the soil is compacted. This concept is shown in Figure 2.

On the wet side of optimum the compacted soil tends to have a dispersed structure. The degree of dispersion of the compacted soil

at a water content on the wet side of optimum increases with increasing shear strain developed during compaction (7). Thus, the compaction method which causes large shear strains produces a high degree of dispersion. Increasing degrees of dispersion at water contents wet of optimum are produced by static, dynamic, and kneading methods of compaction respectively.

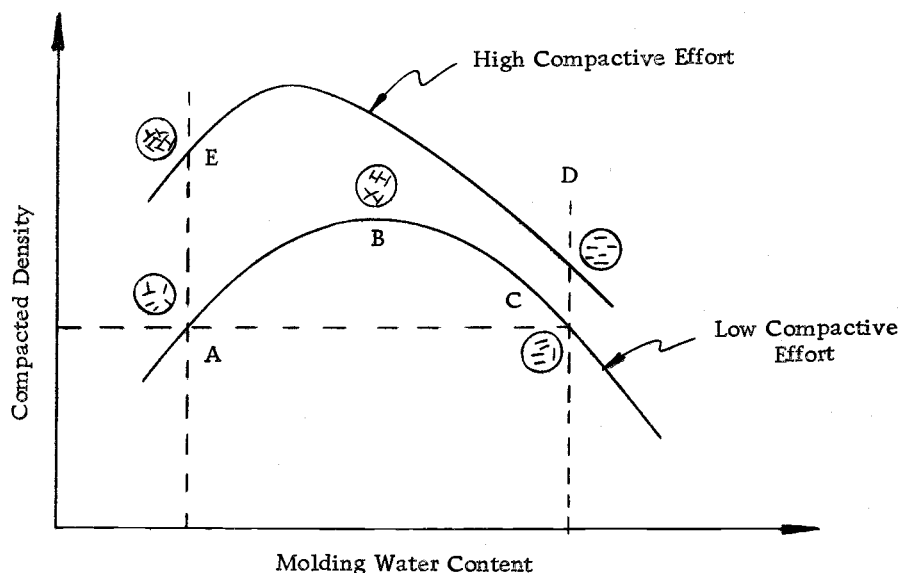


Figure 2. Effects of compaction on structure. (After Lambe, 1958).

### Effect of Soil Structure on Soil Properties

Differences in soil structure resulting from compaction can have a pronounced effect on the engineering properties of a soil. It was observed by Seed and Chan (7) that samples compacted dry of optimum shrink appreciably less than those compacted wet of optimum. From the data obtained during the same study the more flocculated

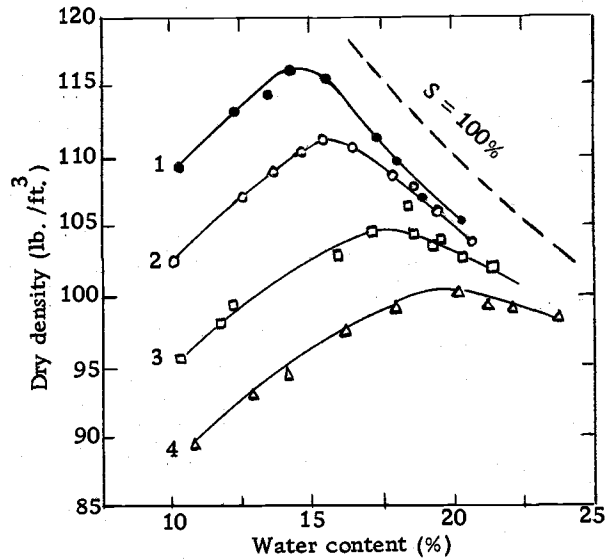
samples have much steeper stress-strain curves and develop their maximum strengths at low strains. The more dispersed samples have much flatter stress-strain curves and continue to increase in strength even at high strains.

Compacted soil strength in terms of effective pressures is not influenced by soil structure (7).

#### Effect of Mode of Compaction

Different compactive energies produce different relationships between moisture and density. This can be seen from the work of Turnbull (11) in Figures 3 and 4. Figure 3 shows the results of laboratory tests using dynamic compaction. The soil was compacted using different compactive efforts. The compactive effort was increased from test 4 through test 1. As the data illustrate, for a given type of compaction the higher the compactive effort the higher the maximum density and the lower the optimum water content. Further, as the molding water content increases, the influence of compactive effort on density tends to decrease. The points of maximum dry density and optimum water content for the various compactive efforts tend to fall along a line that goes in the same general direction as the lines of constant degree of saturation.

Figure 4 shows the results of static compaction in which the compacting stress is decreased going from test 1 toward test 4. As



No.	Layers	Blows per Layer	Hammer Weight	Hammer Drop
1	5	55	10 lb	18 in. (mod. AASHO)
2	5	26	10	18
3	5	12	10	18 (std. AASHO)
4	3	25	5-1/2	12

Note: 6 in. diameter mold used for all tests.

Figure 3. Dynamic compaction curves for a silty clay.  
(From Turnbull, 1950).

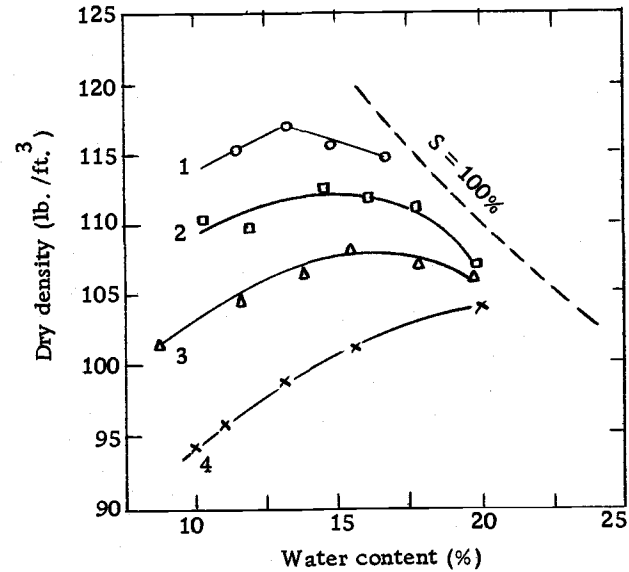


Figure 4. Static compaction curves for a silty clay.  
(1) 2000-psi static load. (2) 1000-psi static load. (3) 500-psi static load. (4) 200-psi static load. Note: Compaction on top of soil samples. (From Turnbull, 1950).

illustrated in the figure, the higher the compactive stress the higher is the maximum density.

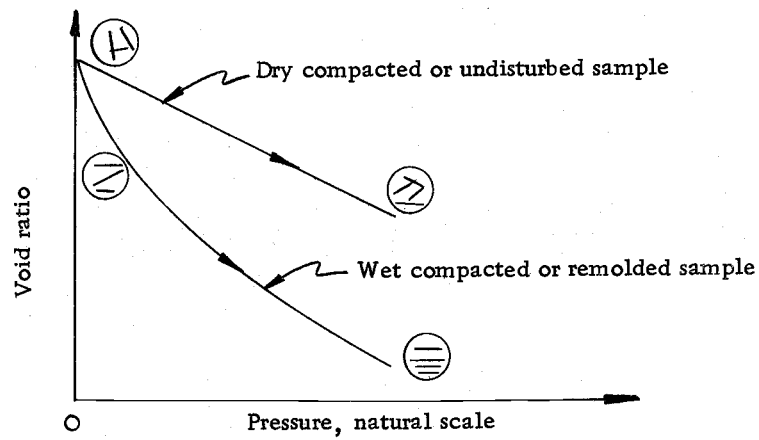
The method of compaction that produces large shear strains during compaction, causes a more orderly array of soil particles. From this observation it is evident that different methods of compaction produce different strengths of compacted soils since the dispersed structure is not as strong as the flocculated.

#### Influence of Compaction on Compressibility of Soil

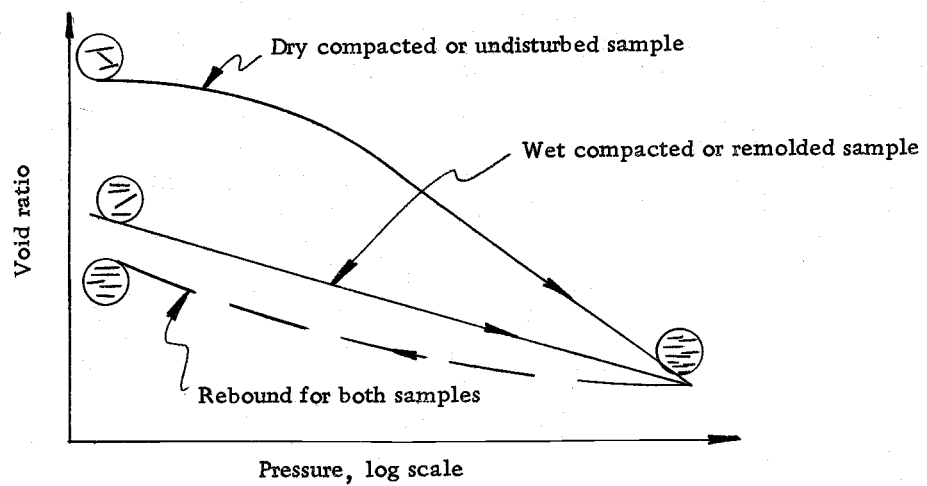
The compressibility characteristics of compacted cohesive soil were studied by Lambe (2). He used the one-dimensional compression method for his tests. His results are conceptually presented in Figure 5.

Figure 5 illustrates the differences in compression characteristics between two saturated clay samples at the same density, one compacted on the dry side of optimum and the other compacted on the wet side. At low pressure (Figure 5-a), the wet side compacted sample is more compressible than the dry side sample since the flocculated particles have more resistant to compression. After the applied pressure becomes great enough to cause particle reorientation, the compression of the dry side and wet side compacted samples are approximately equal. At high applied pressures (Figure 5b)

the sample compacted on the dry side is more compressible than the sample compacted on the wet side.



(a) Low pressure consolidation.



(b) High pressure consolidation.

Figure 5. Effect of one-dimensional compression on structure. (After Lambe, 1958).

## LABORATORY STUDIES

### General

To determine the orientation of soil particles after compaction there are both direct and indirect methods. For this study linear shrinkage measurements were taken from air-dried cubical samples trimmed from compacted specimens. The cubical samples were cut at various directions from direction of compression ( $\alpha = 0^\circ, 18^\circ, 36^\circ, 54^\circ, \text{ and } 90^\circ$ . See Figure 6). In addition, the compression indices ( $C_c$ ) from one-dimensional compression tests on samples with various directions of loading to the direction of compaction were compared to study the effects of arrangement of particles. The rheological constants of the soil were determined from one-dimensional compression test results.

Laboratory tests were performed in the Department of Civil Engineering Soils Laboratory, Oregon State University during the fall term of 1970.

The soil tested (10) was a plastic sandy silt (MH) having a liquid limit, LL, of 64% and a plasticity index, PI, of 19%. The specific gravity of the soil was 2.77. The moisture density relationship for the soil determined by ASTM Standard Test D-698 is shown in Figure 7.

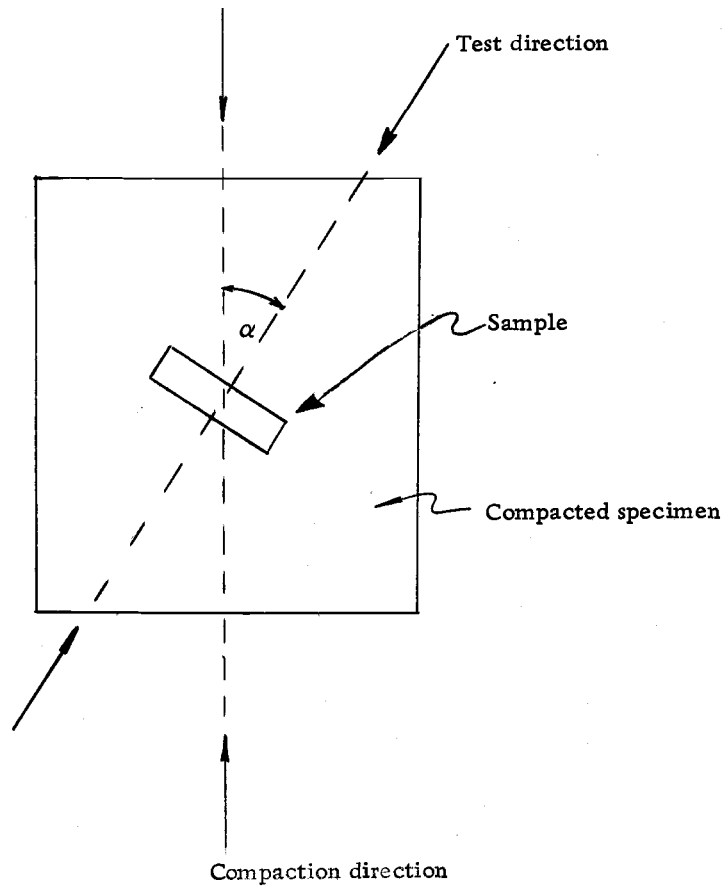


Figure 6. Test sample orientation.

The test samples were mixed with predetermined amount of water to achieve optimum moisture content plus three percent. After mixing, the soil was stored overnight in a closed container in a humid room to improve the uniformity of the water content of the mix.

After one night of storage, the soil was compacted in the four inch standard mold by the kneading method. The samples for linear shrinkage measurements and one-dimensional compression were trimmed from this compacted specimen.

### Test Procedure

#### Linear Shrinkage Test

Cubical samples were cut from six compacted specimens at various angles,  $\alpha$  (see Figure 6). Using the device shown in Figure 8 three dimensions of the samples were measured and the soil was weighed to find the relationship between water content and shrinkage. The dimensions were measured to  $1 \times 10^{-4}$  inches accuracy. Weight was determined to  $1 \times 10^{-4}$  grams. During the first three days, measurements were taken twice a day; after that they were taken once a day. While the test was being performed the cubical samples were kept in a container to inhibit drying. The specimens dried in the oven after the shrinkage was nearly complete. The dry weight was obtained and the relationship between water content and shrinkage

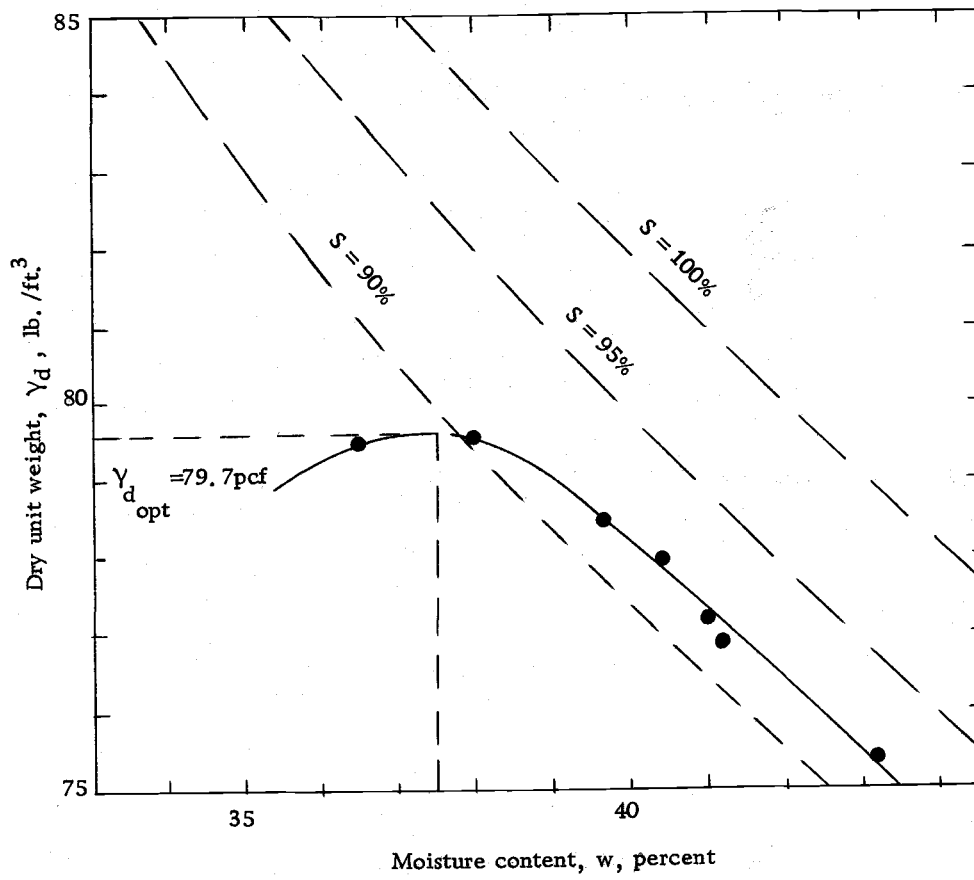


Figure 7. Moisture density relationship.(After Steward, 1971).

was plotted as shown in Figure 11.

### One-dimensional Compression Test

The samples for this test were prepared from the compacted specimens. Again the angles,  $\alpha$ , were  $0^\circ$ ,  $18^\circ$ ,  $36^\circ$ ,  $54^\circ$ ,  $90^\circ$ , and  $0^\circ$  as for the cubical samples.

After the test samples were obtained, the initial weights of the ring (1.0" x 2.5" dia.) and specimen were recorded. Saturated porous stones were fitted to the top and bottom of the specimen before placing the assemblage in a lucite dish. Water was then poured into the dish to the level of the bottom stone. The dish was sealed by using plastic to prevent evaporation during testing. Then the loading head was adjusted above the sample, and the deflection dial set. A load increment ratio of one was used in these tests and each load was left on for 24 hour duration. Dial readings were taken at various time intervals for each load increment. Loading was started at a pressure of  $0.125 \text{ kg./cm.}^2$  and terminated when a pressure of  $16 \text{ kg./cm.}^2$  was reached. To apply the load to the specimen the Conbel device was employed (Figure 9). The readings were taken to  $1 \times 10^{-4}$  inches.

At the completion of each test, the sample was removed from the loading head and weighed. The initial water content was established from the oven-dried weight and pre-test weight of the soil and ring. For each pressure increment the strain at 24 hour loading was

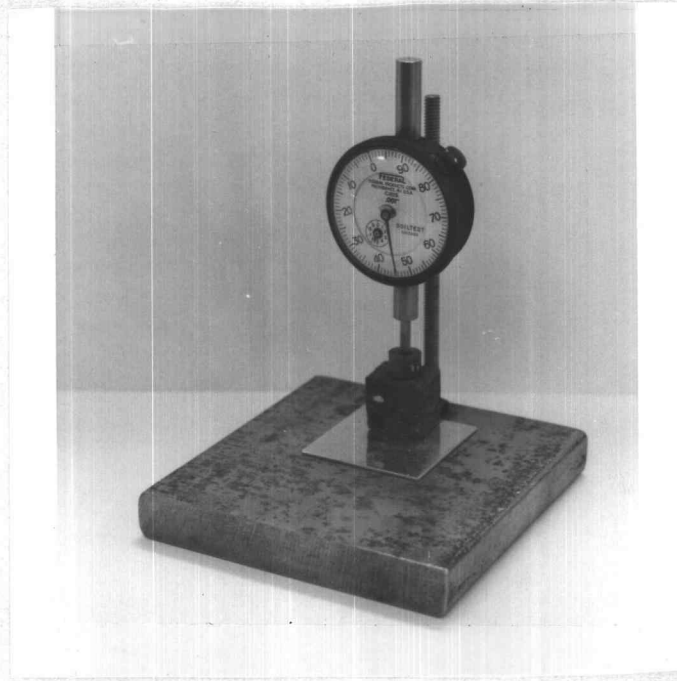


Figure 8. Shrinkage measurement device.

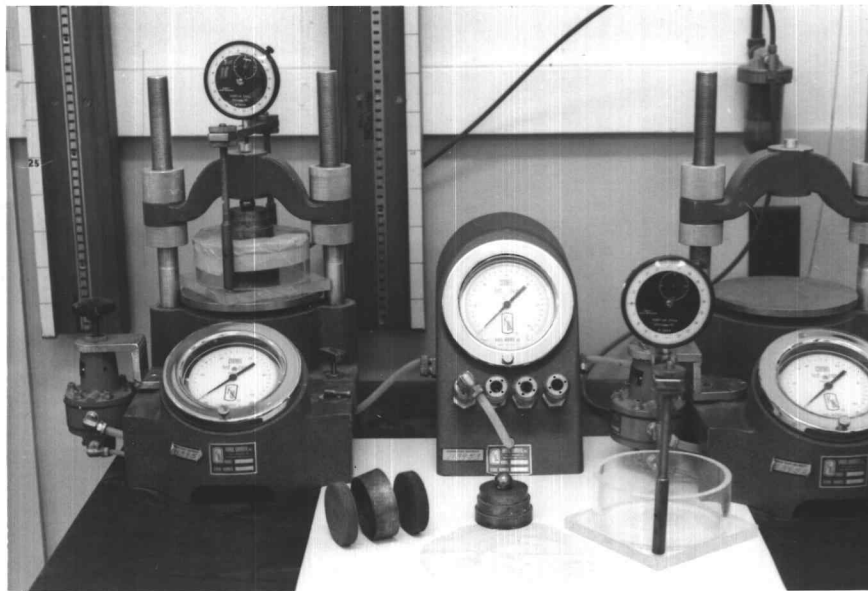


Figure 9. Conbel compression machine.

calculated. The compression index for each angle  $\alpha$  was determined by plotting this strain against the logarithm of the pressure (Figure 12).

The Kelvin rheological model (Figure 10) was fitted to the time-compression data for the soil and the constants  $K$  and  $\eta$  were computed for each data point during a load cycle.

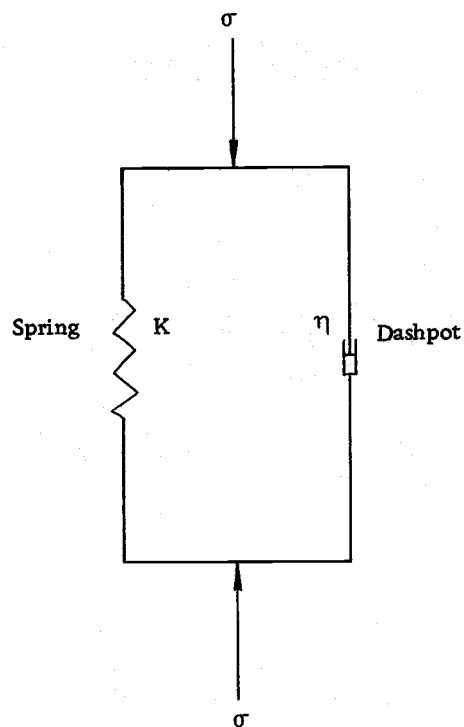


Figure 10. Mechanical model representing soil behavior.

## TEST RESULTS

The results of laboratory tests performed on cubical samples are plotted in Figure 11. The strains at 24 hour for each increment load from one-dimensional tests were plotted against the applied load as shown in Figure 12. The compression indices,  $C_c$ , were computed from the slope of virgin part of each curve in Figure 12 and are shown in Figure 13. They do not significantly vary with the direction of loading. It thus appears that the stress-strain relationship is independent of direction of loading within accuracy of the test.

The soil behavior was thought to be represented by the mechanical model shown in Figure 10. The rheological constants,  $K$  and  $\eta$ , were computed using Equation 2. The spring constant is an isotropic property and is stress dependent (Figure 15). The dashpot constant is also isotropic, independent of stress and is dependent upon time (Figure 16). It thus is not a constant in the strict sense of the word, but using the computed value at any time the strain-time relation may be predicted.

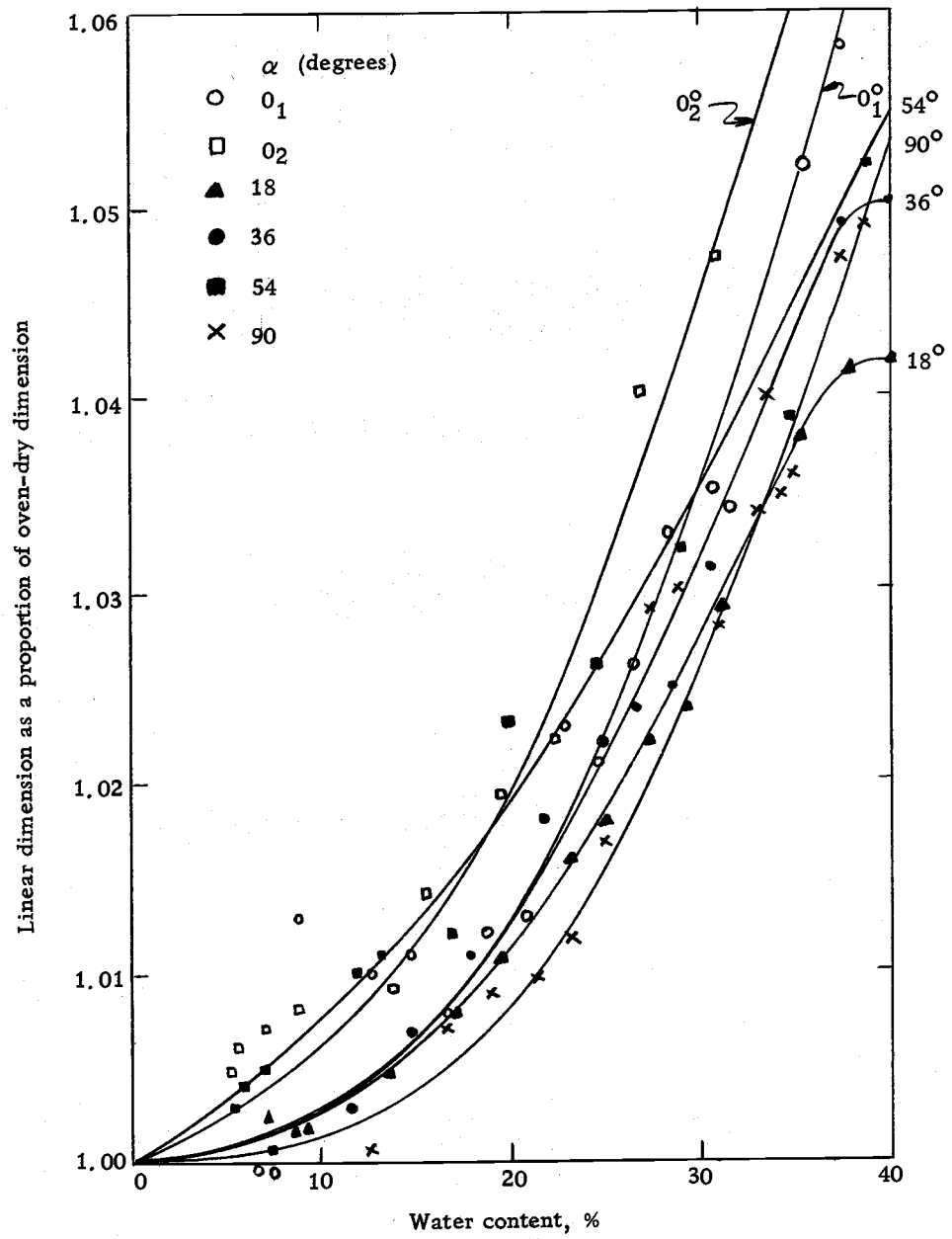


Figure 11. Linear shrinkage test results.

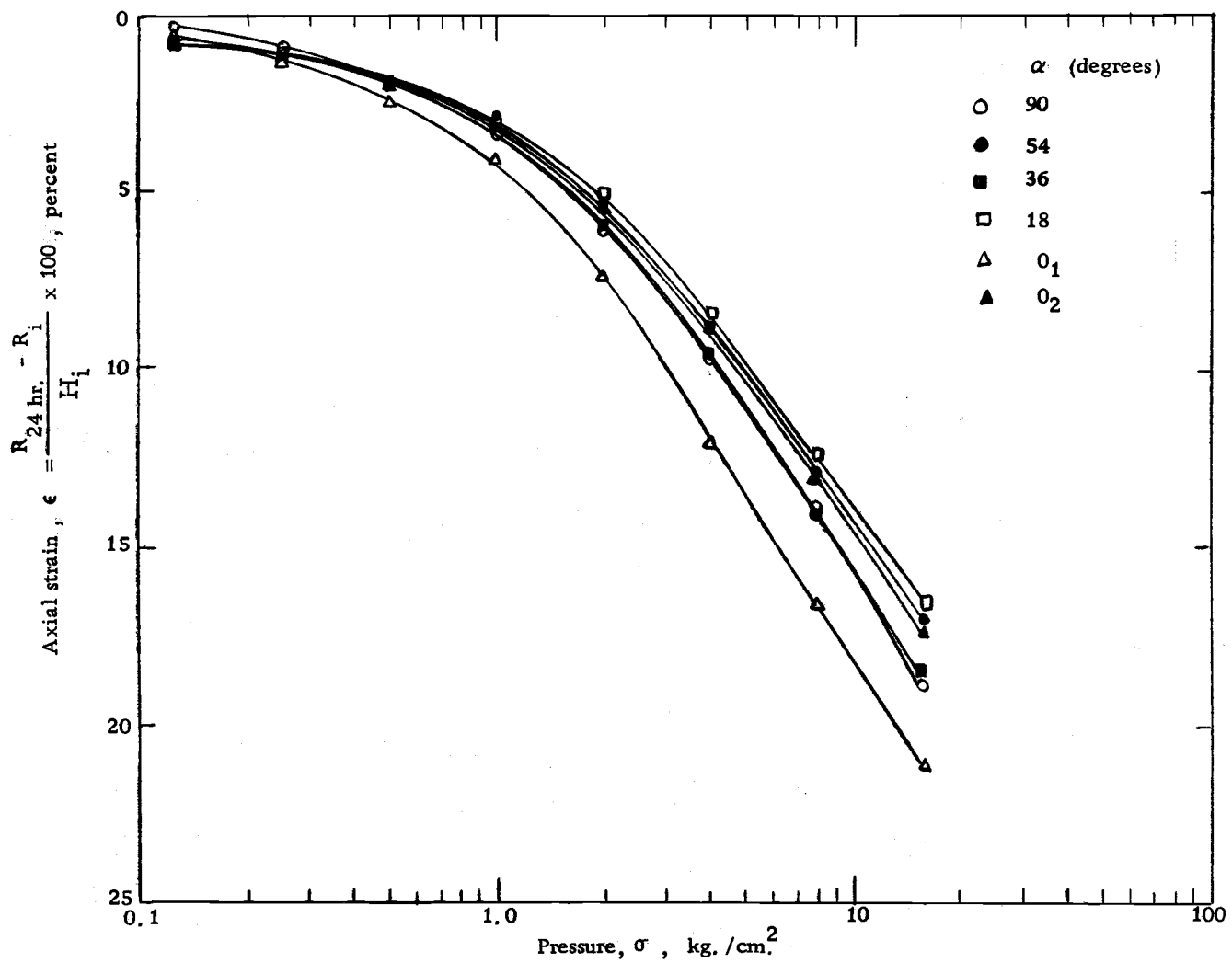


Figure 12. Axial strain versus pressure curves.

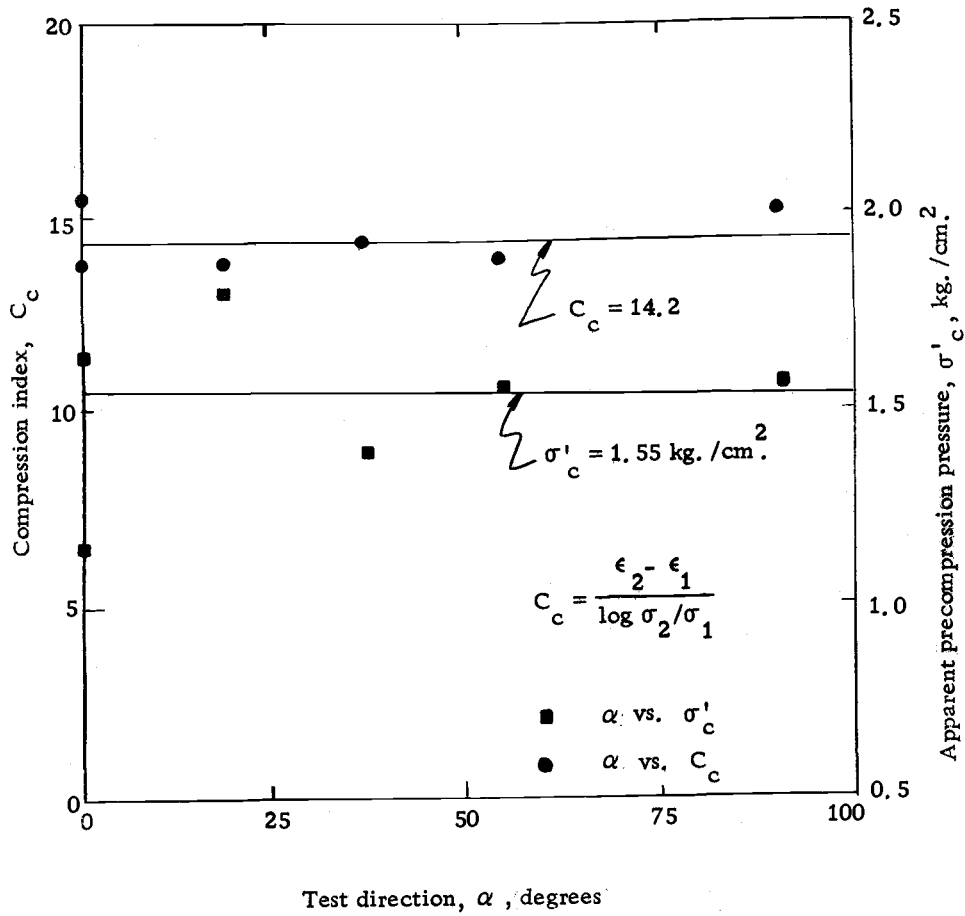


Figure 13. Variation of compression index and apparent precompression pressure with test direction.

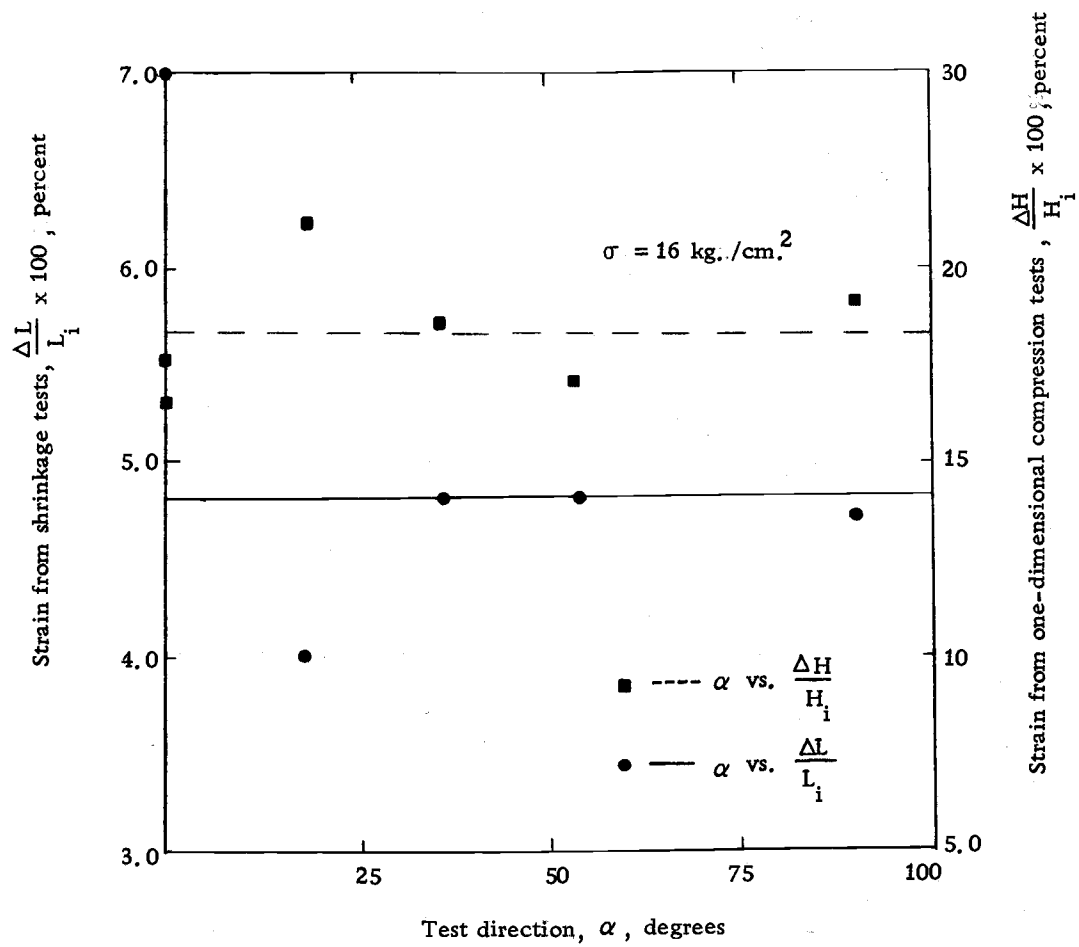


Figure 14. Variation of strain from shrinkage and one-dimensional compression tests with direction of compression.

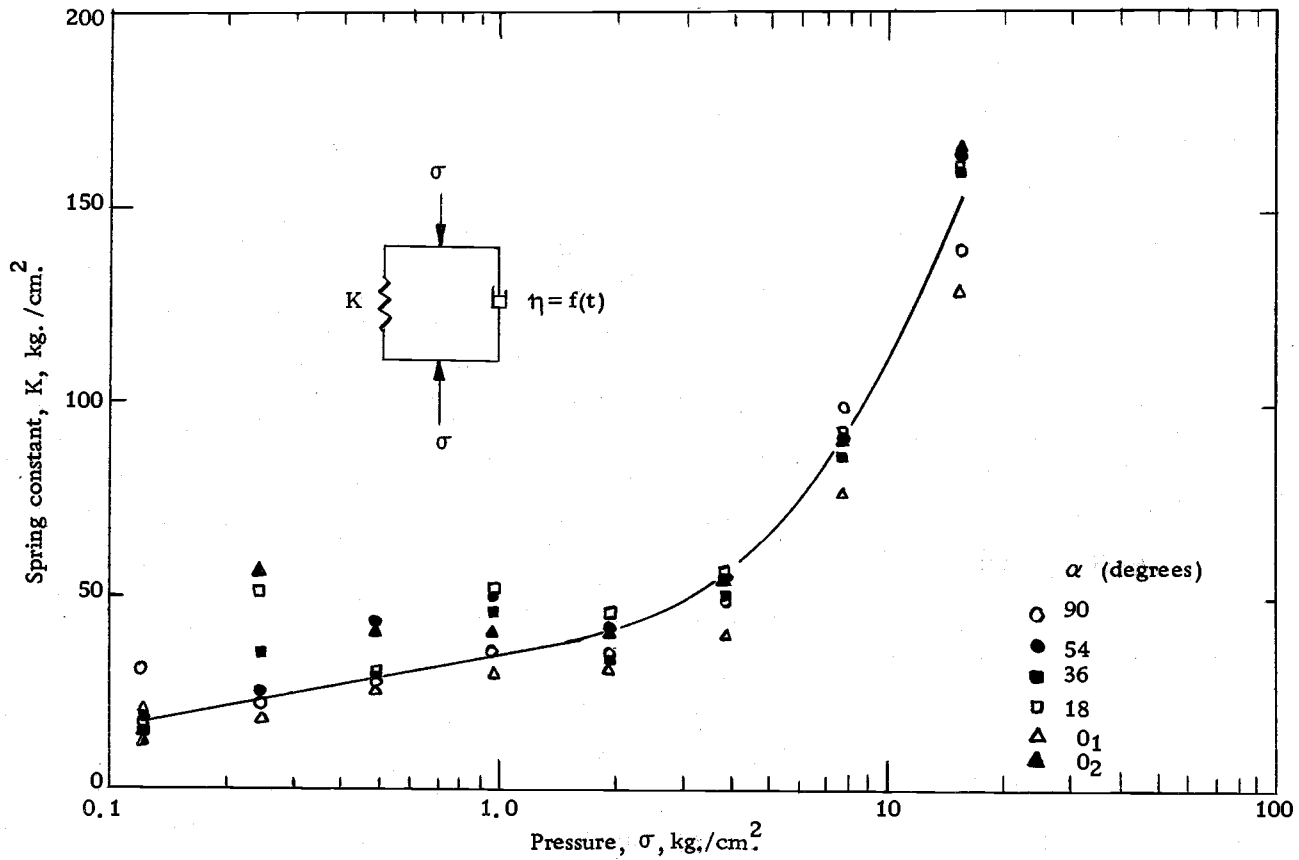


Figure 15. Spring constant variation with pressure.

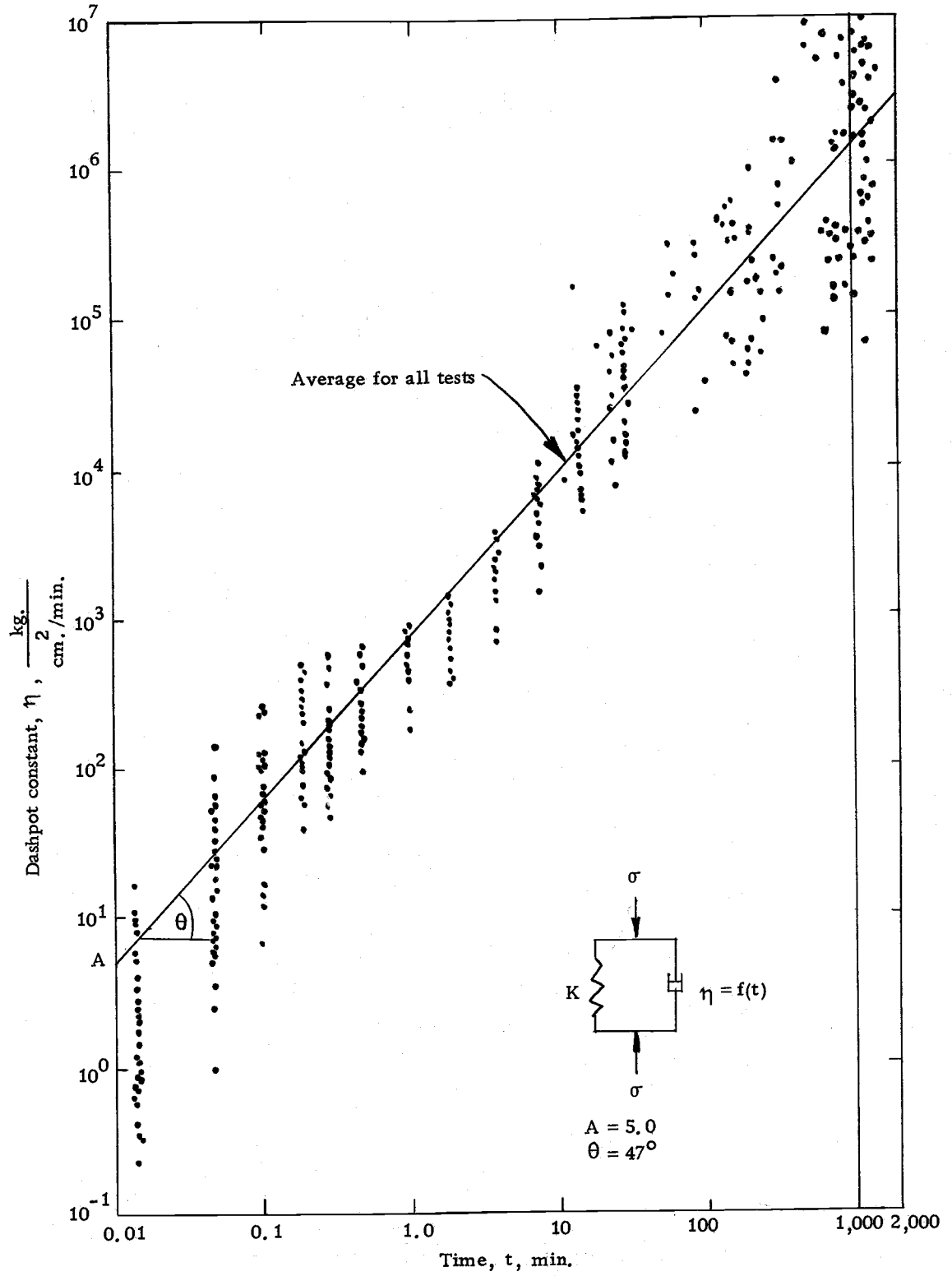


Figure 16. Dashpot constant variation with time .

## DISCUSSION OF RESULTS

### Linear Shrinkage Test Results

The data from the linear shrinkage tests is plotted in Figure 11. The shrinkage was calculated and the dimension relative to the oven dry dimension was plotted against the water content. The particle orientation for each compacted specimen was assumed to be the same since they were compacted by the same energy and at the same moisture content. The shrinkage was measured in the same direction as compression for one-dimensional compression tests. For the dispersed structure of cohesive soil shrinkage will be greater in the direction perpendicular to the plane of the particles even if a water film of uniform average thickness surrounds the particle. This occurs because the proportion of water to solid is greater along a line in this direction. In addition, interparticle repulsion is greater between flat surfaces, resulting in a large average distance between flat surface than between edges.

From Figure 11 it is obvious that the shrinkage does not vary consistently with water content for each direction of compression. This may be interpreted to indicate that the structure of the specimens tend to be flocculated (isotropic) even though they were compacted by kneading at optimum moisture content plus three percent. This

observation is confirmed by the results from one-dimensional compression tests as plotted in Figures 12, 13 and 14, and discussed in the following section.

### One-dimensional Compression Tests

#### Relation between $C_c$ and $\alpha$

Figure 12 is the plot between strain ( $\epsilon$ ) of the sample and log. of applied pressure for six samples compressed in various directions ( $\alpha$  varied). The strain was defined by the following equation:

$$\epsilon = \frac{R_{24 \text{ hr.}} - R_i}{H_i} \times 100 \% \quad (1)$$

in which

- $R_{24 \text{ hr.}}$  = dial reading at 24 hour after increment pressure applied.
- $R_i$  = initial dial reading for first load increment.
- $H_i$  = initial height of test samples
- $\epsilon$  = axial strain in percent.

There are no significant differences among the curves. The compression index ( $C_c$ ) of each specimen was calculated and plotted against the direction of compression as shown in Figure 13. From the figure there is no significant variation between  $C_c$  and  $\alpha$ . This result supports the conclusion derived from shrinkage tests showing

isotropic behavior. In the same figure the apparent precompression,  $\sigma_c^1$ , was plotted against the test direction ( $\alpha$ ). Again a horizontal straight line was obtained.

The relation between total strain from both compression and shrinkage tests and the direction of compression is shown in Figure 14. The strains from shrinkage tests represent shrinkage from the initial water content, the water content of the compression specimen, to a totally dry condition whereas the strain from compression tests is that obtained at constant pressure ( $\sigma = 16 \text{ kg./cm.}^2$ ).

#### Stress-strain-time Relationship

The stress-strain-time relationship of the soil was investigated by representing the soil with the mechanical model shown in Figure 10. The model consisted of a spring and a dashpot connected in parallel. The values of the constants in the model were calculated using the computer program shown in the Appendix, based on the following equation:

$$\epsilon = \frac{\sigma - \eta \dot{\epsilon}}{K} \quad (2)$$

where

$\sigma$  = applied pressure

$K$  = spring constant

$\eta$  = dashpot constant

$\epsilon$  = axial strain

$\dot{\epsilon}$  = strain rate

The spring constant is independent of time and is defined as the ratio of applied pressure to final strain. When plotted against applied pressure (Figure 15) the curve is similar to the familiar  $e - \log. \sigma$  curve. The slope of the curve was constant up to 2 kg./cm.<sup>2</sup>. It then increases gradually to 8 kg./cm.<sup>2</sup> pressure. From that point another higher constant slope was observed. The spring constant behaves isotropically, for all practical purposes.

For each applied pressure the dashpot constant of the soil varied with elapsed time as shown in Figure 16. The straight line in Figure 16 was the average of the straight line from each  $\alpha$  value. The relationship between time and the dashpot constant from Figure 16 is

$$\log \eta = \log A + \left(\log \frac{t}{t_A}\right)(\tan \theta) \quad (3)$$

or

$$\eta = A \left(\frac{t}{t_A}\right)^{\tan \theta} \quad (4)$$

in which

$\eta$  = dashpot constant

$A$  = intercept of the line on log.  $\eta$  axis.

$t$  = instantaneous time

$t_A$  = time at  $\eta = A$

$\tan \theta$  = slope of the line

The strain can thus be predicted by employing equation (4) with

equation (2).

From Figure 16 the deviation of the data points from a straight line was very large in the lower and higher ranges of elapsed time. This has relatively insignificant effect on the strain computed by equation (2). At small values of time, i. e., 1 or 3 seconds, the accuracy of dial reading from which strain is computed is questionable so the average may be considered reasonably valid. When the elapsed time was greater the rate of strain was lower and tends to zero when the sample is completely consolidated. Therefore, the term  $\frac{\eta \dot{\epsilon}}{K}$  was not significant compared to  $\frac{\sigma}{K}$  in the computation of  $\epsilon$ .

Figure 17 shows the linear relationship between strain rate and time. The slope of the lines increases with increasing applied pressure and tends to converge. The relation of strain rate to applied pressure at constant time for several times was observed and plotted in Figure 18. The curves were concave downward at low pressure and convex downward at high pressure. At intermediate pressures the strain rate varies linearly with pressure. When the time is greater the concave part is larger and linear part is shorter. The slope of the linear range decreases as time increases.

The comparison of this study (one-dimensional compression) and triaxial test results obtained by Singh and Mitchell (9) is shown

in Figures 19 and 20. Note in Figure 20 the abscissa of (a) is in arithmetic scale while in (b) it is logarithmic.

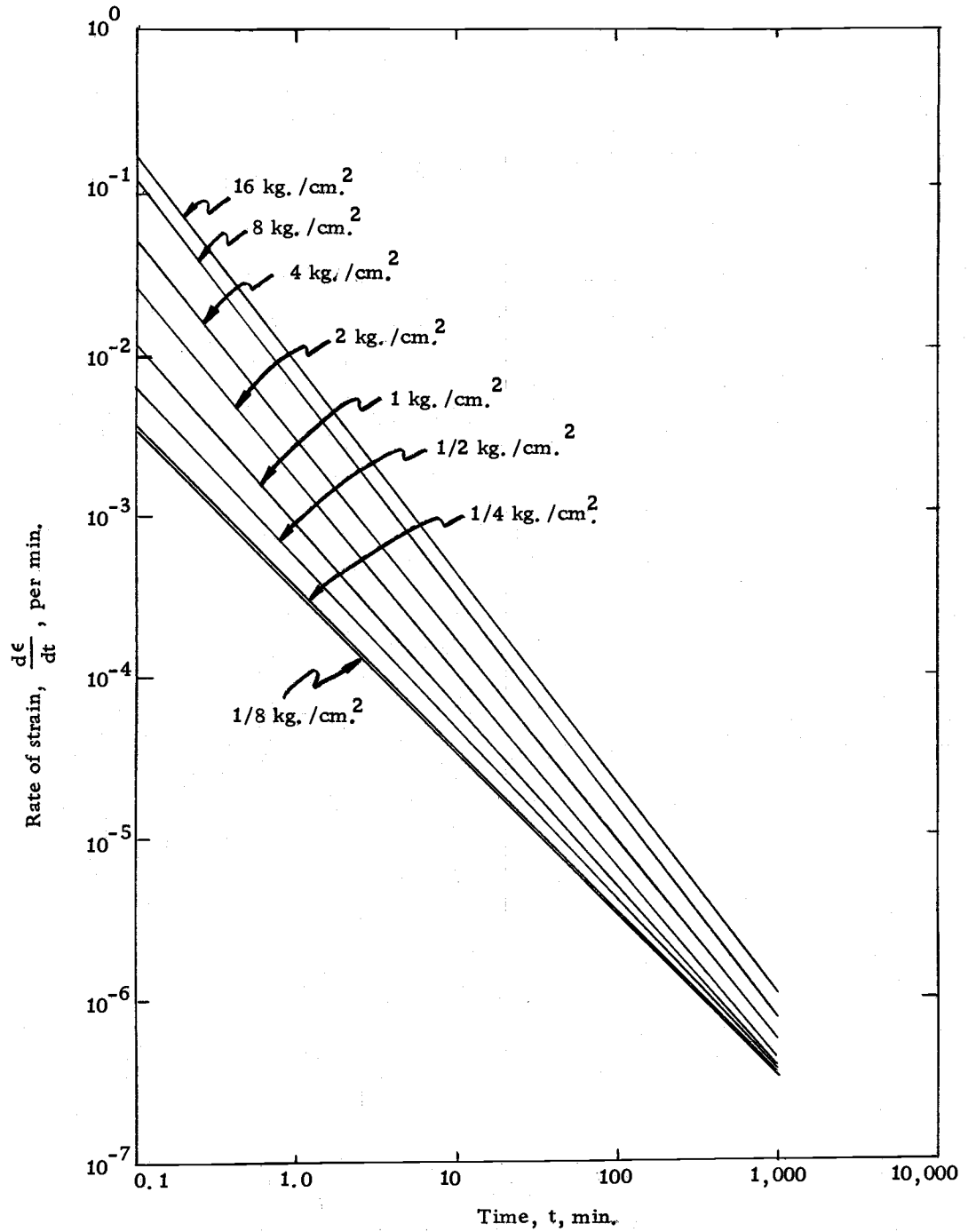


Figure 17. Strain rate versus time relationship from one-dimensional compression test.

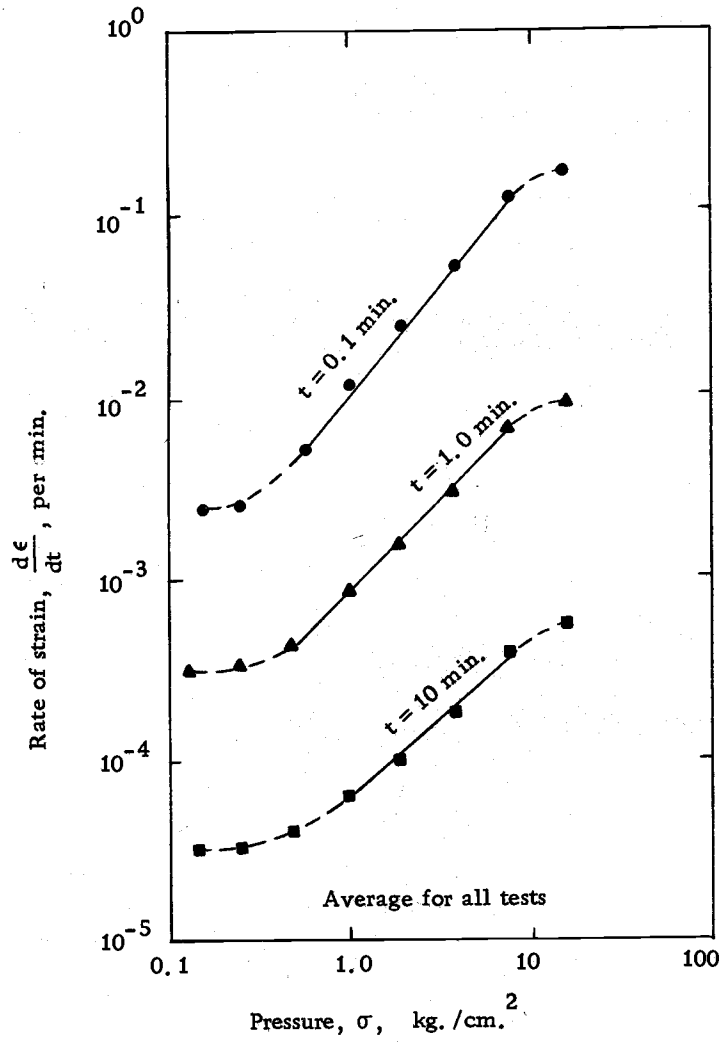
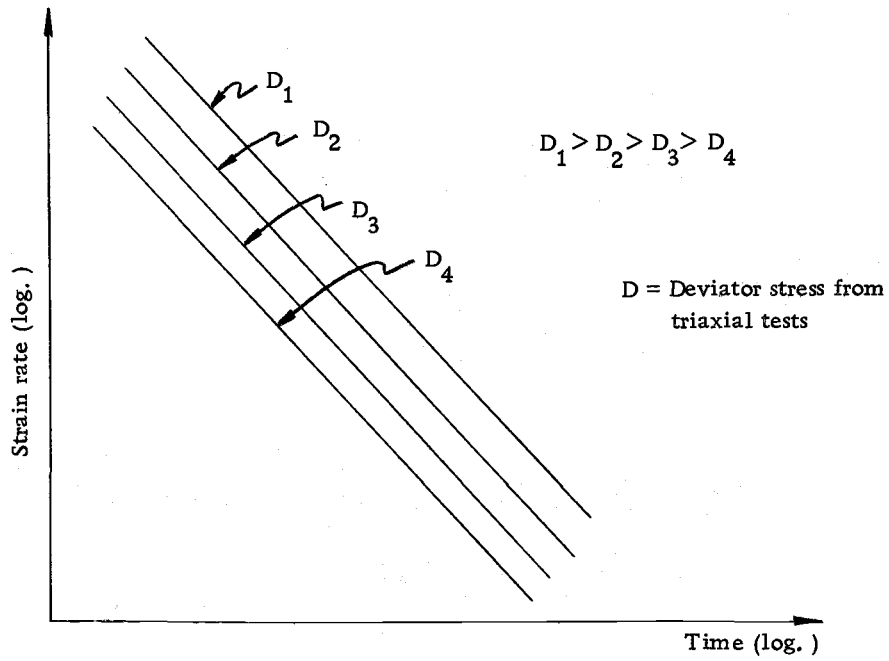
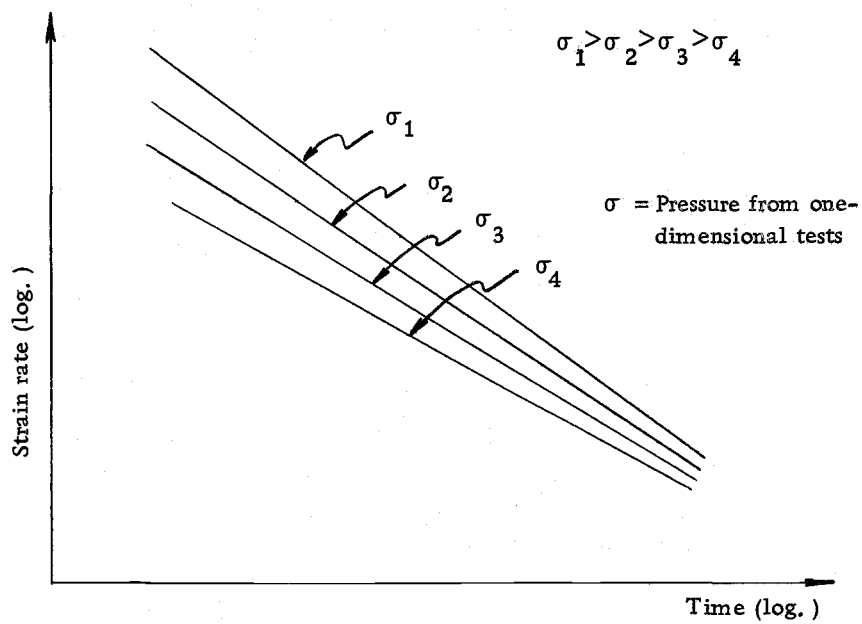


Figure 18. Variation of strain rate with stress of constant time.

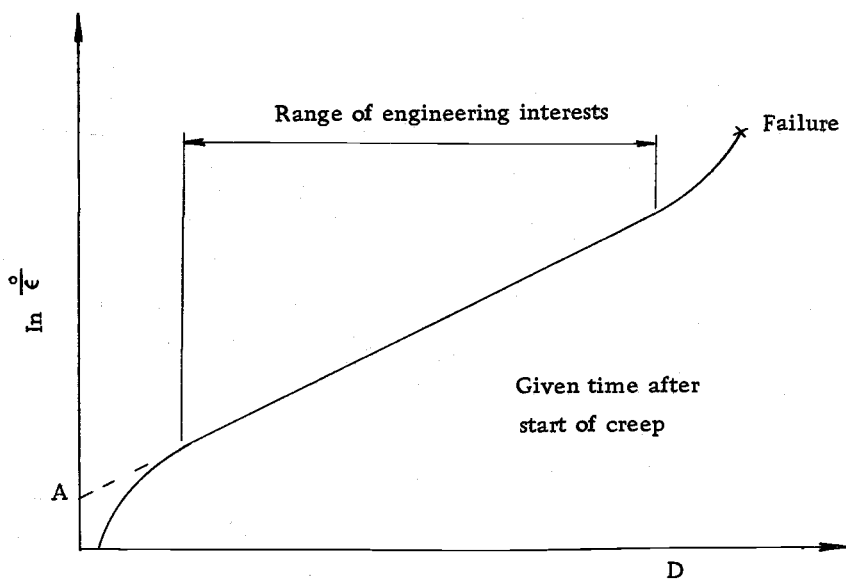


(a) From triaxial test. (After Singh and Mitchell, 1968).

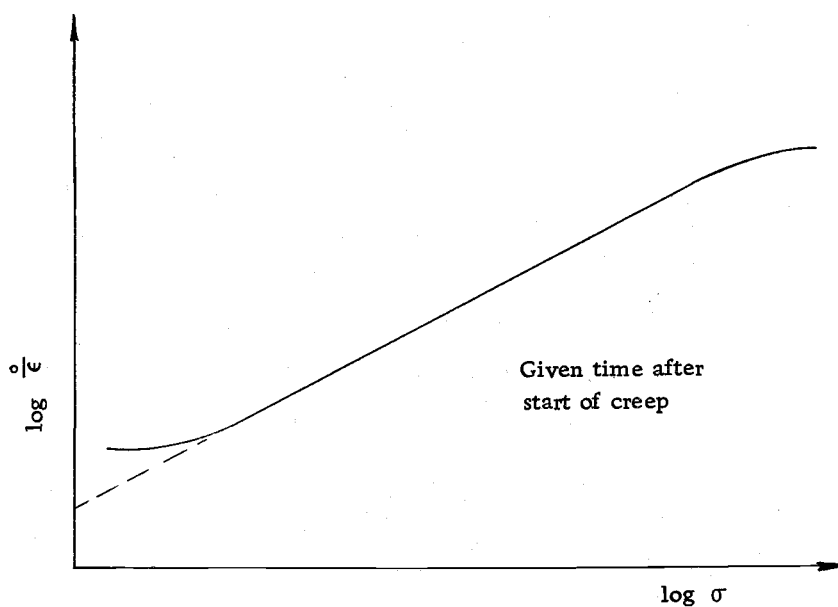


(b) From one-dimensional compression test.

Figure 19. Strain rate-time relationship.



(a) From triaxial test. (After Singh and Mitchell, 1968).



(b) From one-dimensional compression test.

Figure 20. Influence of creep stress intensity on creep rate.

## CONCLUSIONS

The laboratory work was performed to investigate the directional nature of the properties of a compacted soil.

From the test results it can be concluded that:

1. The soil behaves isotropically both with respect to strain and time rate of strain.
2. The spring constant of the soil,  $K$ , varies only as stress is applied.
3. The dashpot constant of soil,  $\eta$ , is independent of the applied stress and is time dependent.
4. Two equations are proposed for the prediction of the stress-strain-time relationship. They are

$$\epsilon = \frac{\sigma - \eta \dot{\epsilon}}{K} \quad (2)$$

and

$$\eta = A \left( \frac{t}{t_A} \right)^{\tan \theta} \quad (4)$$

## BIBLIOGRAPHY

1. Lambe, T. William. 1951. Soil testing for engineers. New York, Wiley. 165 p.
2. Lambe, T. W. 1960. The structure of compacted clay and the engineering behavior of compacted clay. Transactions of the American Society of Civil Engineers 125:682-756.
3. Lambe, T. W. and Robert V. Whitman. Soil mechanics. New York, Wiley. 545 p.
4. Langfelder, L. J. and V. R. Nivargikar. 1967. Some factors influencing shear strength and compressibility of compacted soils. Highway Research Record 235:13-26.
5. Liveh, M. and A. Komomik. 1967. Anisotropic strength of compacted clays. In: Proceedings of the Third Asian Regional Conference on Soil Mechanics and Foundation Engineering, Haifa, 1967. Vol. 1. Haifa. p. 298-304.
6. Pagen, C. A. and B. N. Jagannath. 1968. Mechanical properties of compacted soils. Highway Research Record 235:13-26.
7. Seed, H. B. and C. K. Chan. 1961. Structures and strength of compacted clays. Transactions of the American Society of Civil Engineers 126:1344-1425.
8. Seed, H. B., J. K. Mitchell and C. K. Chan. 1960. The strength of compacted cohesive soils. Proceedings of the American Society of Civil Engineers on Research Conference on Shear Strength of Cohesive Soils, Boulder, Colorado, 1960. p. 877-964.
9. Singh, A. and J. K. Mitchell. 1968. General stress-strain time function for soils. Journal of the Soil Mechanics and Foundations Division, American Society of Civil Engineers 94:21-46.
10. Steward, J. E. Numerical method for calculating construction pore pressure in embankments. Master's thesis. Corvallis, Oregon State University, 1971. 91 numb. leaves.

11. Turnbull, W. J. Compaction and strength tests on soil. In: Soil Mechanics, by J. W. Lambe and Robert V. Whitman. New York, Wiley, 1969. p. 516.
12. Yong, R. N. and Benno P. Warkentin. 1966. Introduction to soil behavior. New York, Macmillan. 451 p.

## APPENDIX

## LIST

```

00001:    PROGRAM KELVIN
00002:C    PROGRAM FOR CALCULATING THE KELVIN MODEL CONSTANTS
00003:    DIMENSION TIME(25)
00004:    1 ,DIREAD(25), DREAD(25), ST(25)
00005:    1 ,STRA(25), DACON(25)
00006:    REWIND 50
00007:    X = TTYIN (4HTEST,4H NAM,4HF...)
00008:    ALPHA = TTYIN (4HALPH,3HA= )
00009:    SIGMA = TTYIN (4HLOAD, 4H INC, 4HREME,4HNT I, 4HN KG,4H/SQC,
00010:    1 3HM = )
00011:    N = TTYIN (4HDATA, 4H SET,4HS = )
00012:    DO 15 I = 1, N
00013:    READ (60,10) TIME(I), DIREAD(I)
00014: 10  FORMAT (F10.0, F10.0)
00015: 15  CONTINUE
00016:    DO 30 I = 1, N
00017:    DREAD(I) = DIREAD (I)/10000.
00018:    ST(I) = (DREAD(I) - DREAD(1))/(1.0 - DREAD(1))
00019: 30  CONTINUE
00020:    SPCON = SIGMA/ST(N)
00021:    STRA(1) = 0
00022:    DACON(1) = 0
00023:    DO 40 I = 2, N
00024:    STRA(I) = (ST(I) - ST(I - 1))/(TIME(I) - TIME(I - 1))
00025:    DACON(I) = (SIGMA - SPCON * (ST(I) - ST(I - 1))/2.)/STRA(I)
00026: 40  CONTINUE
00027:    WRITE (61, 45) SPCON
00028: 45  FORMAT (//2X 'SPRING CONSTANT = ',F8.3,
00029:    1 ' KG/SQCM')
00030:    WRITE (61, 50)
00031: 50  FORMAT (//5X'TIME'5X'DIAL READ STRAIN'6X'STR RATE' 4X
00032:    1 'DASH CONST')
00033:    WRITE (61, 55)
00034: 55  FORMAT (5X'(MIN)'6X'(INCHES)'16X'(1/MIN)'3X'KG/SQCM-MIN')
00035:    DO 65 I = 1, N
00036:    WRITE (61,60) TIME(I), DREAD(I), ST(I), STRA(I), DACON(I)
00037: 60  FORMAT (/ ,F12. 4, F12. 5, F12. 6
00038:    1 , 2(E12. 4))
00039: 65  CONTINUE
00040:    END

```